Bio-Inspired Shark Skin Riblets for Centrifugal Pump Impellers: CFD and Experimental Analysis

R. J. Pawar*, M. P. Ray , S. R. Suryawanshi

Department of Mechanical Engineering, MET's BKC Institute of Engineering, Nashik.
SPPU Pune, INDIA

ABSTRACT: This study aimed to investigate a new bionic approach to analyze a centrifugal pump through numerical simulations and compare the results with experimental findings. A centrifugal pump consisting of six backward-curved blades; models of the impeller were designed using the riblet structure of shark skin. The flow inside the pump was studied using *k*-epsilon (*k*-?) turbulence models. The *k*-model gave resul*ts* closest to the real experimental data. In most studies, only design parameters are considered during computational fluid dynamics (CFD) analyses without consideration of experimental results. Here, a new bio-inspired technique called bionics is applied to the impeller of a pump. The experiments were carried out using a computer-controlled testing setup. The pump's performance parameters were analyzed using both CFD simulations and experimental tests on the duty point as per the manufacturer's catalog, having a revolution of 2,900 rpm. The bionic impeller achieves a best efficiency point (BEP) at a discharge rate of 12 m³/hr, with a head of 32.75 m and an efficiency of 39.21%. The CFD results closely matched the experimental results at the design flow rate and at all other tested flow rates. In addition, by integrating nature-inspired design with testing, this study contributes to the development of high-performance, sustainable pumps..

KEYWORDS: Centrifugal pump, Biomimetic riblet structure, Shark skin, CFD

[Received Jul. 10, 2025; Revised Sep 27, 2025; Accepted Oct. 27, 2025] Print ISSN: 0189-9546 | Online ISSN: 2437-2110

I. INTRODUCTION

Centrifugal pumps are widely used for water supply, industrial use, wastewater handling, water treatment, irrigation, and other purposes (Sahoo and Guharoy, 2009). A slight improvement in pump efficiency is possible to reduce the current 20% power consumption relationship of pumps worldwide (Hieninger et al., 2021). There are basically two major issues in the world that has to be addressed: lack of energy and deterioration of the environment. These issues make it more important than ever to improve the energy efficiency of the industry (Liu et al., 2021). An area where a major improvement can be achieved is the operation of the centrifugal pump. These pumps are commonly used in hydroelectric power plants and in many industrial processes. They play an important role in liquid transfer but also use a lot of energy. This means that even a slight improvement in efficiency can save a significant amount of energy. Centrifugal pumps are popular because they are cheap and flexible enough to be used. However, most current designs focus solely on hydraulic performance (how well the pump moves the liquid) or acoustic performance (the amount of noise in the pump) (Dai et al., 2021). These two factors are usually treated as separate concerns, with little effort to optimize them together. This leaves room for improvement.

An exciting field of innovation is biomimetic design systems inspired by nature. Scientists in particular have looked into how shark skin reduces resistance in the water. Shark skin has a small, ribbed structure called riblet, which helps sharks move through the water more easily by reducing resistance (Baeten et al., 2024). This idea is already being utilized in other region, such as the aviation and maritime industries, to enhance efficiency. However, only a limited range of studies have been conducted on riblets; which can improve both the hydraulic and acoustic performance of centrifugal pumps (Dean and Bhushan, 2010). Among tested nonsmoothed vane shapes, the circular pattern showed the best antiwear effect, lowering vane wear while only slightly reducing head and efficiency (Ma et al., 2022)

This study focuses on the use of sharkskin-inspired riblet structures in centrifugal pumps. By adding these riblet structures to the impeller, the goal is to see how they affect the important performance such as pump head (liquid height), power consumption, and overall efficiency (Wang et al., 2024). The study aims to fill a critical gap by not only improving how well the pump moves fluids but also addressing how quiet and efficient it can be at the same time. Numerical simulations have shown that triangular grooves achieve the best noise reduction and velocity between different grooves (Xu et al., 2022). Microstructures with negative crown riblets can effectively reduce drag and flow

*Corresponding author: pawarraj7938@gmail.com

doi: http://doi.org/10.63746/njtd.v22i5.3814

resistance by stabilizing turbulent currents, whereas positive crowns intensify turbulence; therefore, the depth and placement of negative crowns are critical for optimizing drag-reduction performance. (Ao, Wang and Zhu, 2021). Circular micro-grooves on vane surfaces reduced wear by altering particle trajectories, with little impact on hydraulic performance (Ma et al., 2022). Shallow dimples on the suction-side front of blades improved efficiency and reduced drag by stabilizing boundary layers (Liu et al., 2024)

CFD and optimisation enable digital twins for legacy turbines, aiding modernization. It highlighted mesh-independence and turbulence model validation as critical for predicting efficiency, cavitation, and head (Ohiemi and McNabola, 2025). CFD provides inexpensive and accurate variations in scaling model testing, which allows for rapid simulations to be performed (Siddique et al., 2017; Singh et al., 2014). The development of CFDs provides a detailed analysis of the flow structure of the pump (Yedidiah, 2008). CFD (SST k–ω) and experiments to analyze entropy generation in axial turbines, showing that turbulent dissipation is the main loss source and that adding blades reduces overall losses, with CFD results matching experimental pressure data (Ohiemi et al., 2023). In modern technology application, the design and development of mechanical components are increasingly shifting towards virtual platforms. Modern software tools such as CATIA, Autodesk Inventor, Solid Edge, SolidWorks, Siemens NX, and CFturbo are now commonly employed to facilitate this transition (Chandrasekaran et al., 2021). Simulation tools such as ANSYS, AutoCAD, FlexSim, and others are widely utilized to analyze fluid flow behaviour. These tools help validate the performance and innovative aspects of mechanical components. (Gülich, 2010). CFD (SST) with pressure sensor tests, showing rotor–stator interactions drive key pulsations and confirming CFD's reliability through close experimental agreement (Li et al., 2022). Simulation tools offer detailed insights into the internal flow behaviour of pumps, eliminating the immediate need for physical testing on actual equipment. They also allow analysis of various boundary conditions influencing pump performance. For instance, using ANSYS, by changing the number of impeller blades and the angle at which they exit, one can study how these changes affect the pump's efficiency and the pressure it produces (Sankar, 2018). Numerous investigations have concentrated on analyzing the flow patterns and pressure profile within the pump system, especially in impellers and spiral housing areas. However, numerical models' reliability confirmation, i.e., experimental review remains problematic (Hassan, Abdallah et al., 2016). Numerical models of pumps in the ANSYS program were compared with experimental measurements in wheel innovation (Alemi et al., 2015). In this study, numerical models were checked using available experimental data; the model's results can be effectively compared with real-world observations, often showing strong correlation. Parameters such as pressure and flow rate of liquids can be reliably measured using devices like pressure gauges and flow meters (Deshmukh et al.,2017).

Centrifugal pumps are critical for industrial water transport, yet those operating at 10 m³/h and 2900 rpm often exhibit high start-up noise, indicating inefficiencies in impeller design and power usage. This study explores the impact of bionic riblet structures on pump performance.

II. METHODOLOGY

A. Bionic impeller

The subject of this study is a centrifugal pump operating at a constant rotational speed of 2900 rpm. The pump's design flow rate at its operating point is 10 m³/h, with the primary geometric and hydraulic parameters of the impeller detailed in Table 1.

Table 1 Main geometric parameters

Components	Parameters	Symbols	Value	Unit
Impeller	Inlet diameter/mm	D_1	40	mm
	Outlet diameter/mm	D_2	25	mm
	Impeller diameter/mm	D	175	mm
	Blade number	z	6	

Although various bionic groove designs have been explored, research on their effects in centrifugal pumps remains limited. Therefore, this study investigates the influence of shark skin-inspired bionic grooves on the hydraulic performance of centrifugal pumps. Figure 1 shows the Bionic Groove Geometry.

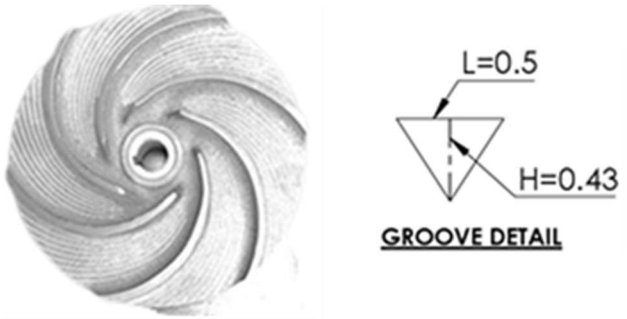

Figure 1 Bionic groove geometry

B. Computational grid design

Grid generation, or meshing, is the process of dividing the flow domain into smaller control volumes. Most studies use unstructured tetrahedral elements for meshing centrifugal pumps (Siddique et al., 2017). Some researchers, for instance, Jafarzadeh et al. (2011) and Hedi et al., (2010) combined structured and unstructured elements, while others Kumar et al. (2013) use a mix of unstructured hexahedral and tetrahedral elements. Some applied tetrahedral grids for the double-volute casing and hexahedral grids for the impeller. In this study, all flow domains were meshed using unstructured tetrahedral grids, which are better suited for handling the complex geometry of the impeller and volute casing (Zhang et al., 2020).

Figure 2 shows the grid of the model which is generated in ICEM CFD software. All domains are generated with unstructured tetrahedral grids. To capture the flow physics more accurately, the impeller domain was refined with a greater number of elements, which improves the reliability of the simulation results. The total number of elements created for the whole model is approximately 2.5 million.

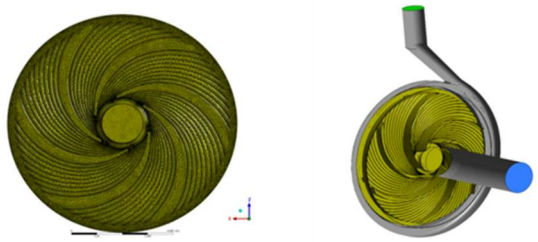

Figure 2 Discretised computational domain

A mesh independence study was carried out with 1.8, 2.5, and 3.4 million elements, refined in the impeller domain. Variations in pressure head, efficiency, and torque between the medium mesh (2.5 million) and fine mesh (3.4 million) were within 1–1.5%, confirming mesh independence. Therefore, the medium mesh was adopted as it provided sufficient accuracy while maintaining computational efficiency, and with residuals below 1.0×10^{-5} (pressure residuals 1.0×10^{-6}), the results are both mesh-independent and numerically robust.

C. Numerical simulation

The Navier–Stokes equations provide a general framework for describing fluid flow. When applied to pumps and other flow machines, the basic Navier–Stokes equations must be adapted to represent the additional complexities introduced by rotation. These include momentum transfer and energy losses in rotating channels, which require modified turbulence models for accurate simulation. To model the flow in pumps more accurately, different turbulence models have been studied, including the SST *k-ω,* and standard *k-ε.* Among these, the *k-ε* turbulence model was determined to be the most suitable for performing Computational Fluid Dynamics (CFD) simulations of the centrifugal pump under investigation.

The impeller domain is modeled as a rotating fluid with water, a rotational velocity of 2900 rpm, isothermal conditions at 25°C, and a *k-ε* turbulence model.

Table 2 Boundary conditions for the present study

Position	**Boundary Condition**
Inlet	Mass flow inlet
Outlet	Pressure outlet
Impeller	Rotating reference frame
Interface	General Connection
Frame	Frozen Rotor
Wall at Casing	No slip Wall

The casing domain is stationary with similar properties and turbulence model. Boundary conditions for the impeller include mass and momentum transfer interfaces, no-slip walls, and smooth wall roughness. The casing inlet has a total pressure of 1 bar, and the outlet specifies a mass flow rate, with no-slip walls on the casing surfaces. This setup ensures an accurate simulation of the fluid dynamics of the centrifugal pump. The boundary conditions used in the analysis were based on real operational conditions, as outlined in Table 2.

The ANSYS CFX software was used to solve flow equations. The transport equations provided below are used to determine the turbulence kinetic energy and its dissipation rate

$$\frac{\partial}{\partial t}(\rho k)+\frac{\partial}{\partial x_i}(\rho k\mu_i)=\frac{\partial}{\partial x_i}\left[\left(\mu+\frac{u_t}{\sigma_k}\right)\frac{\partial k}{\partial x_j}\right]+G_k+G_b-\rho\varepsilon-Y_M+S_k \quad (1)$$

And

$$\frac{\partial}{\partial t}(\rho\varepsilon)+\frac{\partial}{\partial x_i}(\rho\varepsilon\mu_i)=\frac{\partial}{\partial x_j}\left[\left(\mu+\frac{u_t}{\sigma_\varepsilon}\right)\frac{\partial\varepsilon}{\partial x_j}\right]+C_{1\varepsilon}\frac{\varepsilon}{k}(G_k+C_{3\varepsilon}G_b) - C_{2\varepsilon}\rho\frac{\varepsilon^2}{k}+S_\varepsilon \quad (2)$$

Where G_k represents the production of turbulence kinetic energy resulting from mean velocity gradients, calculated according to the approach outlined in the *k-ε* models, G_b is the generation of turbulence kinetic energy due to buoyancy, calculated as described in effects of buoyancy on turbulence in the *k-ε* models, Y_M is the term that accounts for the influence of fluctuating dilatation in compressible turbulence on the overall dissipation rate, evaluated as per the methodology discussed in the *k-ε* models treatment of compressibility effects, $C_{1\varepsilon}$, $C_{2\varepsilon}$ and $C_{3\varepsilon}$ are constants, σ_k and σ_ε are the turbulent Prandtl numbers for k and ε, respectively, and S_k and S_ε are user-defined source terms.

D. Turbulent viscosity representation

The turbulent (or eddy) viscosity is calculated by integrating the effects of various turbulence parameters as follows:

$$\mu_t=\rho C_\mu\frac{k^2}{\omega} \quad (3)$$

Where C_μ is a constant. The model constants. $C_{1\varepsilon}$, $C_{2\varepsilon}$, C_μ, σ_k and σ_ε have the following default values.

$C_{1\varepsilon}=1.44$, $C_{2\varepsilon}=1.92$, $C_\mu=0.09$, $\sigma_k=1.0$ and $\sigma_\varepsilon=1.3$

These default values are based on experimental data obtained from basic turbulent flow scenarios, such as common shear flows—including boundary layers, mixing layers, and jets—as well as from studies of decaying isotropic turbulence generated by grids. They have been found to work fairly well for a wide range of wall-bounded and free shear flows.

E. Experimental setup

The experimental set up shown schematically in Figure 3. The efficiency of a centrifugal pump is evaluated experimentally, focusing on how varying flow rates influence key performance parameters. The flow rate is controlled by adjusting the discharge valve, gradually reducing the effective diameter of the pump's discharge pipe from an initial size of 0.40 meters to near closure. Before initiating the pump operation, the elevation head is measured by determining the vertical distance between the reservoir water level and the discharge pipe centerline using a tape measure. During operation, elevation head variations are monitored using a vertical scale, with efforts made to maintain a consistent elevation head throughout the experiment.

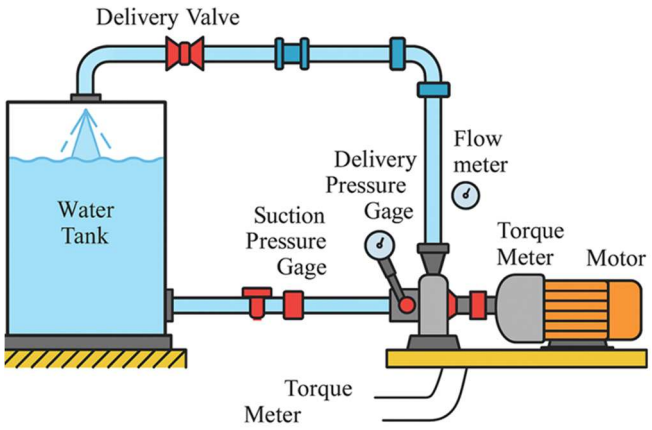

Figure 3 Centrifugal pump test rig block diagram

To assess pump performance, key parameters such as input power, pressure head, and rotational speed are recorded. The pump is initially run until a steady-state condition is reached. A variable frequency drive (VFD) is used to measure the impeller's rotational speed in revolutions per minute. The pressure head is recorded using a pressure gauge installed on the discharge line, with readings taken in kg/cm². The input power, representing the electrical energy supplied to the pump, is obtained from the test setup panel, which consists of a voltmeter and an ammeter, providing power consumption values in kilowatts.

Flow rate measurements are conducted using an electromagnetic flow meter, which operates based on the principle of electromagnetic induction. These meters offer highly accurate readings for water-based fluids due to the absence of moving parts, thereby minimizing mechanical wear and measurement errors. To vary the flow rate, the discharge valve is gradually adjusted while keeping the pump speed constant. Five specific operating conditions are selected based on the manufacturer's specifications and in accordance with IS: 13518-1992 standards.

The total head developed by the pump is determined using Bernoulli's principle, which considers the combined effect of elevation head, pressure head, and velocity head. In this study, head losses due to friction and flow disturbances caused by bends and fittings are assumed to be negligible for simplification.

Pump efficiency is evaluated by measuring the volumetric flow rate in six distinct trials, with each trial consisting of two replicates. The average of these replicates is considered for analysis. The output power imparted to the fluid by the pump is calculated using the product of flow rate, fluid density, gravitational acceleration, and total head. The actual power supplied to the pump is obtained directly from the test setup panel. Efficiency is then determined as the ratio of output power to input power, expressed as a percentage.

III. RESULTS AND DISCUSSION

In this study, the performance of a centrifugal pump was investigated through both experimental testing and computational fluid dynamics (CFD) simulations. The operating conditions were selected based on manufacturer specifications, with a constant rotational speed of 2900 rpm. The flow rate was varied by adjusting the discharge valve while maintaining a steady pump speed. Five specific operational conditions were considered for the analysis.

For the CFD simulations, the pump's rotational speed remained fixed while the volume flow rate was systematically varied from 0 to 12 m³/h. After achieving convergence, key parameters such as, turbulence kinetic energy, mass flow rate, turbulence dissipation rate, and velocity profiles were evaluated to ensure that the solution remained within an acceptable convergence criterion of 10^{-4}. Figures 4 a, b, c and

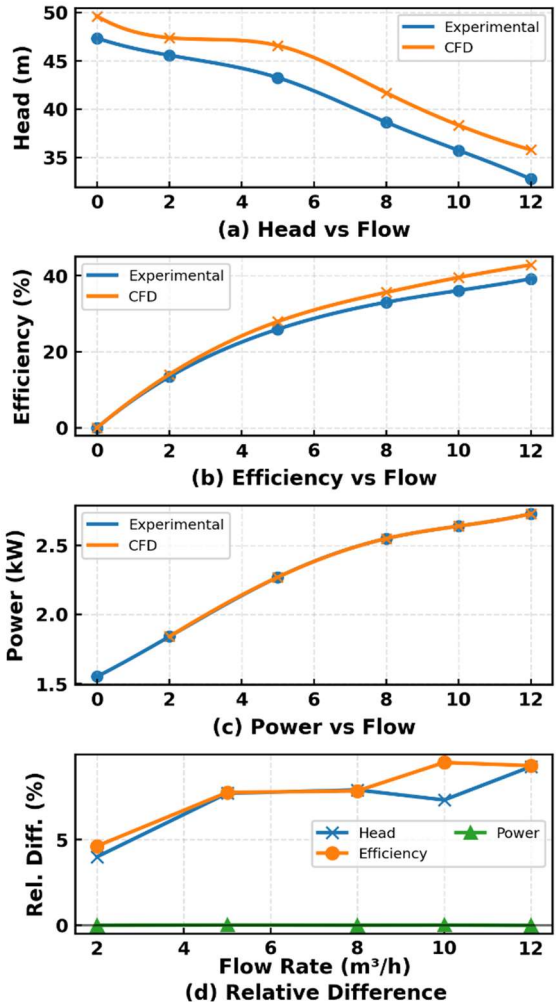

Figure 4 Comparison between CFD simulation and experimental results

d present the comparison between CFD simulation and experimental results of the pump.

The flow analysis was conducted using the *k-ε* turbulence model, which was applied at the design flow rate. When compared with experimental data, the *k-ε* turbulence model provided the most accurate results, demonstrating its effectiveness in predicting the pump's performance.

The simulation employed a fluid–fluid interface under steady-state conditions, with water as the working fluid and a turbulence intensity of 5%. The CFD and experimental findings for pump head and hydraulic efficiency at the design flow rate are illustrated in the figure. A detailed comparison of hydraulic efficiency and head with respect to volumetric flow rate, based on both experimental and numerical data, is depicted in Figures 4(a) and 4(b).

Figure 4(a) compares the head–flow performance curves of the bionic impeller pump obtained from experiments and CFD simulations. As is characteristic of centrifugal pumps, the head is highest at shut-off and declines progressively with increasing discharge. The CFD-predicted head curve aligns closely with the experimental results, demonstrating that the model captures the overall performance trend effectively. At the design flow, the agreement is especially strong, with discrepancies of only 1–2% at the best efficiency point (BEP). Minor deviations appear at the off-design extremes: at very low flow and especially toward the maximum flow (~12 m³/h), the CFD tends to slightly over-predict the head compared to experiment.

Figure 4(b) compares the pump's hydraulic efficiency obtained from experiments and CFD efficiency is low at zero flow, increases with flow, and reaches a peak before declining at the highest flow rates. The peak of this curve identifies the best efficiency point (BEP). In this case, the BEP occurs at approximately Q ≈ 12 m³/h, where the pump achieves its maximum efficiency. At this optimum, the experimental efficiency reaches about 39.21%, while the CFD predicts a slightly higher peak around ~42%. The CFD and experimental efficiency values at the BEP are almost coincident, demonstrating that the simulation accurately pinpoints the optimal operating condition. Overall, the efficiency comparison shows a strong agreement in curve shape and peak location, with only small discrepancies at off-design points.

Figure 4(c) illustrates the pump's hydraulic output power as a function of flow rate. Figure 4(d) illustrates the relative discrepancies between CFD simulations and experimental measurements for head, efficiency, and power across varying flow rates. Near the Best Efficiency Point (BEP), deviations are minimal less than 1% which validates the CFD model's accuracy at the design condition. When the operating point shifts away from the BEP, discrepancies increase, though head differences remain limited to 5–7%. Overall, the CFD results demonstrate reliable accuracy, with all errors remaining below 9%.

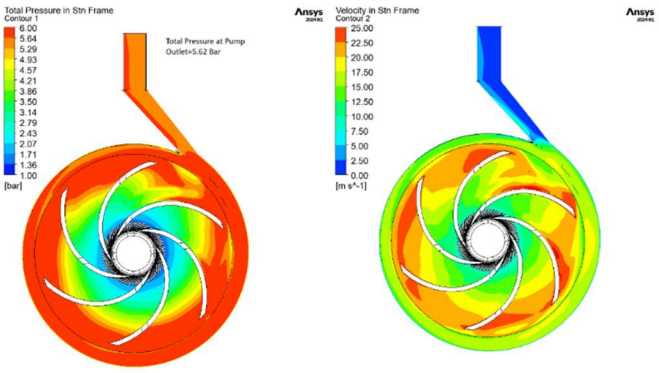

(a)Total pressure contours and velocity contours at a flow rate of 2 m³/h

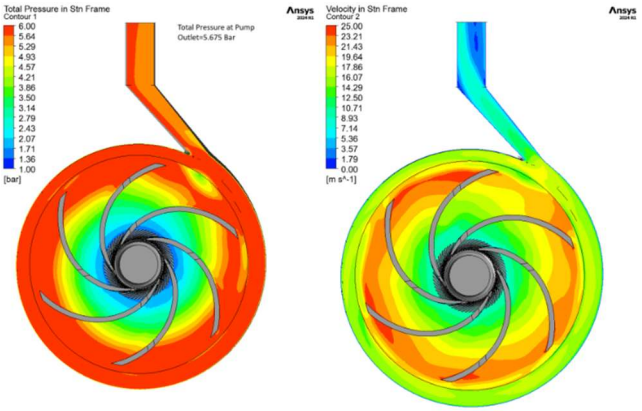

(b)Total pressure contours and velocity contours at a flow rate of 5 m³/h

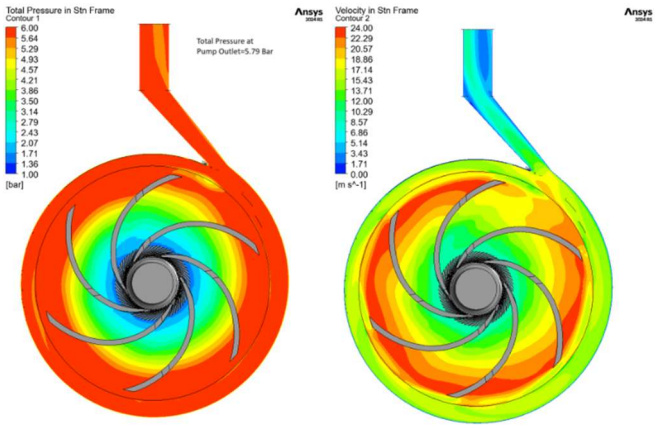

(c)Total pressure contours and velocity contours at a flow rate of 8 m³/h

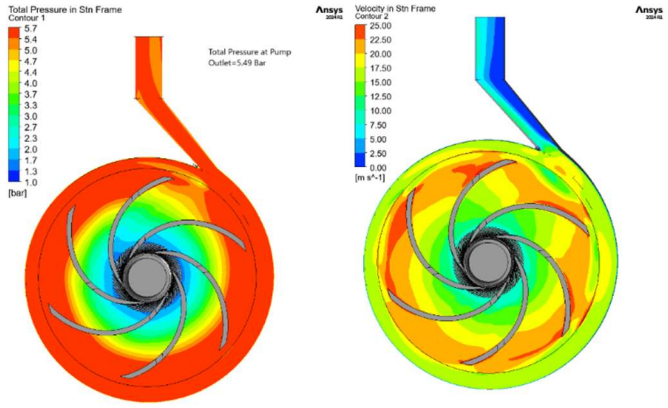

(d)Total pressure contours and velocity contours at a flow rate of 10 m³/h

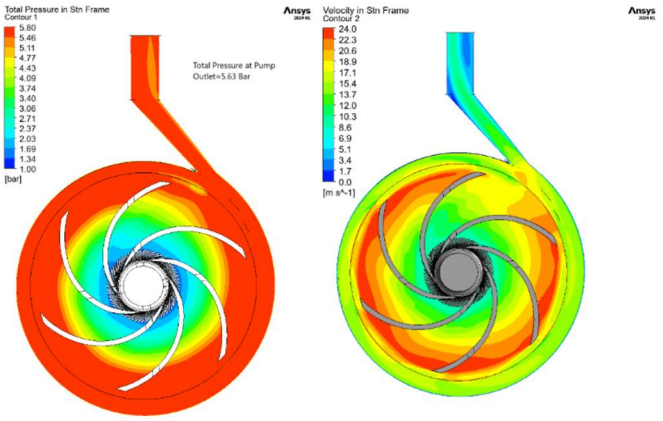

(e)Total pressure contours and velocity contours at a flow rate of 12 m³/h.

Figure 5 Total pressure contours and velocity contours at different flow rates: (a) 2 m³/h, (b) 5m³/h and (c) 8 m³/h (d) 10 m³/h (e) 12 m³/h

Two-dimensional total pressure contours and corresponding velocity contours in XZ cross-section plane are indicated in Figure.5, at low flow conditions, the bionic impeller maintained a stable pressure field, characterized by smooth green/blue gradients, indicating low energy dissipation. The velocity plot showed minimal spikes and steady flow, suggesting reduced turbulence and more efficient energy usage as shown if Figure 5(a).

As indicated in Figure 5 (b) with mid-range flow, the bionic impeller continued to minimize turbulence, showing well-distributed pressure zones and a uniform velocity field. This resulted in better energy conservation and less mechanical wear on internal components. At higher flow conditions, the bionic impeller maintained smoother pressure transitions, reducing high-gradient zones that typically indicate energy loss. Velocity vectors remained well directed and steady, limiting resistance and improving fluid dynamics as presented in Figure 5(c).

With increasing load, the bionic impeller continues to display stable pressure distributions and evenly spread velocity fields. Such characteristics limit hydraulic losses, reduce component stress, and enhance long-term operational reliability. This enhances operational reliability and reduces hydraulic losses in high flow environment as indicated in Figure 5(d). It can be seen in Figure 5(e) that as extreme duty, the bionic impeller continued to exhibit superior pressure handling with stable velocity fields, even under high stress. The bionic impeller sustains performance under extreme flow, reducing cavitation risk and energy loss, ensuring durable and efficient operation.

IV. CONCLUSION

This study presents a comprehensive analysis of CFD simulations and experimental investigations conducted on a centrifugal pump equipped with a bionic impeller. The computational results were validated against experimental data obtained from a physical prototype manufactured by Indo Pump Pvt. Ltd, India. The key enhancements and findings from this research are summarized as follows: (i) The integration of sharkskin-inspired riblet structures into the impeller design significantly improved hydraulic performance, demonstrating higher efficiency, increased head, and reduced energy losses compared to conventional designs; (ii) The computational fluid dynamics (CFD) analysis using the k-ε model closely matched experimental results across all duty points, particularly at the Best Efficiency Point (BEP), with error margins under 2% in critical parameters; (iii) The simulation setup, including boundary conditions and meshing strategy, proved effective in predicting real-world performance, making it a reliable tool for future impeller and pump design validation; (iv) The bionic impeller maintained uniform pressure and velocity distributions even under extreme flow conditions (up to 12 m³/h), thereby enhancing mechanical integrity and minimizing cavitation risks; (v) The bionic impeller design achieved a peak hydraulic efficiency of 39.21% at the design flow rate, contributing to lower power consumption and promoting more sustainable fluid transport solutions in industrial applications; (vi) This study successfully demonstrates the practical application of biomimicry in mechanical systems, bridging nature-inspired innovation with real-world engineering through both simulation and experimental validation; and (vii) The promising results encourage further exploration of bio-inspired geometries for noise reduction, multi-phase flow handling, and advanced impeller materials, paving the way for next-generation energy-efficient pumps.

REFERENCES

Alemi H.; Nourbakhsh S.; Raisee Dehkordi M. and Najafi A. (2015). Effects of volute curvature on performance of a low specific-speed centrifugal pump at design and off-design conditions. *Journal of Turbomachinery,* 137(4), 1-10.

Ao M.; Wang M. and Zhu F. (2021). Investigation of the turbulent drag reduction mechanism of a kind of microstructure on riblet surface. *Micromachines, 12(1)*, 1-13. https://doi.org/10.3390/mi12010059

Baeten SRR; Kochovski A.; Jovanova J. and Sakes A. (2024). Characterization of shark skin properties and biomimetic replication. *Bioinspiration & Biomimetics, 19(5*), 1-16. https://doi.org/10.1088/1748-3190/ad5c25

Chandrasekaran M.; Santhanam V. and Venkateshwaran N. (2021). Impeller design and CFD analysis of fluid flow in rotodynamic pumps *Materials Today: Proceedings,*37(2),2153-2157. https://doi.org/10.1016/j.matpr.2020.07.637

Dai C.; Guo C.; Chen Y.; Dong L. and Liu H. (2021). Analysis of the influence of different bionic structures on the noise reduction performance of the centrifugal pump. *Advances in Mechanical Engineering, 21(3)*, 886–895.

Dean B. and Bhushan B. (2010). Shark-skin surfaces for fluid-drag reduction in turbulent flow: A review. *Philosophical Transactions of the Royal Society A: Mathematical, Physical and Engineering Sciences, 368(1929)*, 4775–4806.

Deshmukh D.; Siddique M.H. and Samad A. (2017). Surface roughness effect on performance of an electric submersible pump. *Proceedings of the ASME 2017 Gas Turbine India Conference,1-10,* ASME

Gülich J. F. (2010). Centrifugal pumps. *Springer Berlin, Heidelberg, (2),* 34-966.

Hassan A.; Abdallah H. and Abou El-Azm Aly A. (2016). Effect of impeller blade slot on centrifugal pump performance. *Global Journal of Research in Engineering, 16(4)***,** 71–85.

Hedi M. L.; Hatema K. and Ridha Z. (2010). Numerical flow simulation in a centrifugal pump. *International Journal of Thermal Technologies,2(4) ,*209-215.

Hieninger T.; Goppelt F.; Schmidt-Vollus R. and Schlücker E. (2021). Energy-saving potential for centrifugal pump storage operation using optimized control schemes. *Energy Efficiency, 14(23)***,** 1-14. https://doi.org/10.1007/s12053-021-09932-5

Jafarzadeh B.; Hajari A.; Alishahi MM. and Akbari MH. (2011). The flow simulation of a low-specific-speed high-speed centrifugal pump. *Applied Mathematical Modelling, 35(1)***,** 242–249.

Kumar S.; Mohapatra S.K. and Gandhi B. K. (2013). Investigation on centrifugal slurry pump performance with variation of operating speed. *International Journal of Mechanical and Materials Engineering, 8(1)***,** 40–47.

Liu H.; Cheng Z.; Ge Z.; Dong L. and Dai C. (2021). Collaborative improvement of efficiency and noise of bionic vane centrifugal pump based on multi-objective optimization. *Advances in Mechanical Engineering, 13(2)***,** 1–15.

Liu J.; Zhang F.; Zhu L.F.; Yuan S.Q.; Xu R.H. and Zhang H. (2024). Influence of bionic structure on hydraulic performance and drag reduction effect of a centrifugal pump. *Journal of Physics: Conference Series, 2707(1)*, 1-18.

Li, Y.; Ohiemi, I.E.; Singh, P.; Sunsheng, Y. (2022). Numerical and experimental analysis of pressure fluctuation in axial flow turbine. *AIP Advances, 12(2),*1-26.

Ma G.; Xia L.; Mou M.; Wu Y. and Yan, Z. (2022). Effect of bionic nonsmooth surface vane on the antiwear characteristics of double-vane pump. *Applied Bionics and Biomechanics, 2022(1)***,** 1-13.

Ma L.; Gu Y.; Xia K.; Mou C.; Mou J.; Wu D. and Yan M. (2022). Influence of bionic circular groove blade surface on wear performance. *Lubricants, 10(5)***,** 1-17.

Ohiemi, I.E.; Cervantes, M.J.; McNabola, A. (2023). Evaluation of energy loss in a low-head axial flow turbine under different blade numbers using entropy production method. *Energy, 263(1) ,*1-20

Ohiemi, I.E.; McNabola, A. (2025). Supporting the digitalisation of existing hydropower plants using CFD modelling. *Renewable Energy, 235(1),*122–138

Sahoo T. and Guharoy A. (2009). Energy cost savings with centrifugal pumps. *World Pumps, 2009(1),* 35–37.

Sankar S. (2018). Analysis of centrifugal pump impeller using ANSYS. *International Journal of Innovative Research in Science, Engineering and Technology, 7(5),* 5021–5026.

Siddique M. H.; Bellary SAI; Samad A.; Kim J. H. and Choi Y. S. (2017). Experimental and numerical investigation of the performance of a centrifugal pump when pumping water and light crude oil. *Arabian Journal for Science and Engineering, 42(11)***,** 4605–4615.

Siddique M. H.; Bellary SAI and Samad A. (2017). Design and optimization of pump impeller using response surface methodology and genetic algorithm. *Design Engineering, 2017(28),*147–155.

Singh V. R.; Zinzuvadia M. J. and Sheth SM. (2014). Parametric study and design optimization of centrifugal pump impeller – a review. *International Journal of Engineering Research and Applications, 4(1),* 216–220.

Wang Y.; Dong L.; Zhou R.; Guo C. and Dai C. (2024). Energy loss and noise reduction of centrifugal pump based on bionic V-groove geometry. *Water, 16(15)***,** 2183–2195.

Xu Z.; Liu X.; Liu Y.; Qin W. and Xi G. (2022). Flow control mechanism of blade tip bionic grooves and their influence on aerodynamic performance and noise of multi-blade centrifugal fan. *Energies, 15(9)***,** 3431. https://doi.org/10.3390/en15093431

Yedidiah S. (2008). A study in the use of CFD in the design of centrifugal pumps. *Engineering Applications of Computational Fluid Mechanics, 2(3),* 331–343.

Zhang H.; Tang L. and Zhao Y. (2020). Influence of blade profiles on plastic centrifugal pump performance. *Advances in Materials Science and Engineering, 2020(1),*1–17. https://doi.org/10.1155/2020/6665520